Original Article

Birnur Akkaya*, Recep Akkaya and Ayşe Hümeyra Taşkın Kafa

Antimicrobially effective protein-loaded metal chelated chitosan composite

https://doi.org/10.1515/polyeng-2023-0060
Received March 15, 2023; accepted June 26, 2023;
published online August 1, 2023

Abstract: The immobilization of lysozyme onto a novel synthetic metal chelator composite based on chitosan/PAA-PMA (chitosan/acrylamide-maleic acid) and its effect on antimicrobial activity were the aim of the current study. The plain composite and the lysozyme immobilized composite were characterized according to scanning electron microscopy (SEM), Ultraviolet spectroscopy (UV), Fourier transform infrared (FT-IR), and X-ray diffraction (XRD) analysis. Furthermore, the activities of lysozyme and immobilized lysozyme were investigated, as well as their antimicrobial activity against *Escherichia coli, Klebsiella pneumoniae, Pseudomonas aeruginosa, Enterococcus faecalis*, and *Staphylococcus aureus*, as well as their cytotoxic effects, which were both approximately greater than those of free lysozyme. The last step was cytotoxic studies on lysozyme, chitosan composite, and lysozyme-immobilized chitosan composite, which showed no cytotoxic effect. Several investigations have shown that metal chelators improve lysozyme's antibacterial action. Two carboxylic acids containing maleic acid were used as a metal chelator in this study. Lysozyme was immobilized from a side other than carboxylic acids, so that carboxylic acid groups, which are metal chelating groups, do not prevent synergy by competing with metal binding at neutral pH. This enhanced antimicrobial activity.

Keywords: antibacterial activity; chitosan; cytotoxic effect; lysozyme; metal-chelating

***Corresponding author: Birnur Akkaya**, Department of Molecular Biology and Genetics, Science Faculty, Sivas Cumhuriyet University, Sivas 58140, Türkiye, E-mail: bakkaya@cumhuriyet.edu.tr, pergamonchem@gmail.com
Recep Akkaya, Department of Biophysics, Medical Science Faculty, Sivas Cumhuriyet University, Sivas, Türkiye
Ayşe Hümeyra Taşkın Kafa, Department of Microbiology, Medical Science Faculty, Sivas Cumhuriyet University, Sivas, Türkiye

1 Introduction

Eating nutritious meals is a requirement for staying healthy throughout life. Food shelf life is shortened due to improper processing and microbial contamination, which increases the risk of foodborne illness. Antimicrobial compounds can be used to inhibit the development of bacteria on food surfaces by immersing, spraying, or brushing them on. However, implementing these strategies is complex and necessitates large concentrations of antimicrobial agents in meals. Loading natural antibacterial compounds into packaging materials, known as "active packaging," is a novel approach to preserving food safety and extending shelf life. Lysozyme is one of the most essential natural preservatives and a natural antimicrobial protein generated from egg white proteins. It is found in a wide range of animals, plants, and microbes and is a strong contender for antibacterial applications in the food and healthcare industries. Food packing and preservation with lysozyme offer greater protection against germs and enhance customer pleasure. Lysozyme, on the other hand, is far more costly than conventional synthetic preservatives, restricting its use. Furthermore, Gram-positive bacteria are extremely susceptible to lysozyme, which has no discernible bacteriostatic impact on Gram-negative bacteria. Several methods have been explored to increase the activity of enzyme molecules and transform lysozyme into a Gram-negative bacteria-killing agent [1]. One of the useful methods is that the attachment of enzymes to nanoparticles is substantially quicker and more practical than the previously discussed approaches, while also lowering uncertainty. Adsorption of enzymes is the most straightforward technique of immobilization. On the other hand, lysozyme is a monomeric protein that may be employed in medicine [2,3] and the food business, but its practical utility is restricted due to its limited antibacterial range, instability, and ease of inactivation [4].

There are a lot of natural polysaccharide studies about lysozyme adsorption, immobilization, or conjugation [5], and one of them is chitosan [6–8].

Chitosan is a biocompatible and environmentally friendly polymer with inherent antibacterial qualities [9].

It is widely utilized in biomedicine, food packaging, and environmental conservation [10]. Rapid dissolution in acidic solutions and poor mechanical properties necessitate improving chitosan packaging properties by modification of chitosan [11–16].

A synthetic metal chelator, ethylenediaminetetraacetic acid (EDTA), is commonly used in food to prevent oxidative deterioration and boost the effectiveness of antimicrobials like lysozyme. By removing membrane-stabilizing cations and/or securing significant nutrients (like iron), metal chelators may improve food antibacterial action (e.g., magnesium, calcium). The antimicrobial synergy of lysozyme and EDTA against *Escherichia coli* and *Listeria monocytogenes* has been widely investigated, and it is generally known that lysozyme and EDTA have a high antimicrobial synergy [17–23]. There is also a lot of research about improving antimicrobial activity of lysozyme and synthetic materials [24–31]. Non-migratory metal chelating active packaging has recently been created as a potential replacement for synthetic metal chelators. Due to covalent attachment to the packaging, notification of food interaction as opposed to immediate clearing of additives would be required for this sort of packaging, which might make it safe for use with both organic and natural goods. Polyacrylic acid, which contains carboxylic acid groups, has been used as a chelator in the literature [32–34]. In the same manner, maleic acid contains dicarboxylic acid groups and is used for heavy metal binding [35,36].

The goal of this study was to look into the influence of antimicrobial activity on chitosan composites by introducing metal chelating properties (increasing carboxylic acid groups by maleic acid incorporation) and using them in combination with lysozyme immobilization.

2 Materials and methods

2.1 Materials

Chitosan (Mw 150000 Da 85 % deacetylated). Lysozyme enzyme powder obtained from the protein of chicken egg whites with specific activity of 40000 U/mg and *Micrococcus lysodeikticus* in the form liofilized powder were purchased from Sigma Aldrich (Germany). An *N*-Ethyl-*N*′-(3-dimethylaminopropyl)carbodiimide hydrochloride, (EDAC, EDC, EDC hydrochloride), 1-Hydroxy-2,5-pyrrolidinedione, N-Hydroxysuccinimide (NHS) and all other reagents (analytical grade) were obtained from Merck (Darmstadt, Germany).

2.2 Composite experimental design

2.2.1 Chitosan composite synthesis: A synthesis of composite studies was performed by Akkaya et al. in a previous study [37].

2.2.2 Lysozyme immobilization: Adsorption is commonly regarded as the most appealing and successful method of enzyme immobilization. In actual applications, this immobilization approach cannot prevent enzyme aggregation on the support. Protein-polysaccharide conjugates are produced as a result of the covalent attachment of polysaccharides to lysozyme by condensation between the carbonyl groups at the reducing end of polysaccharides and the unprotonated amino groups in lysozyme. Covalent cross-linking chemicals (EDC, EDAC) can immobilize enzymes on supports, resulting in more stable contacts between enzymes and carriers [38]. In the current study, EDAC was used to activate lysozyme and couple chitosan amino groups. For the preparation of lysozyme-immobilized chitosan composite, carbodiimide chemistry was applied as follows: lysozyme (10 mg/mL) was mixed with 0.1 M EDAC and 0.1 M NHS. To obtain the lysozyme-immobilized chitosan composite, the activated lysozyme was mixed with chitosan composite after forming the activated ester [8]. The reaction mixture was then sonicated in an ultrasonic environment. After discarding the supernatant to eliminate nonspecifically bound lysozyme, the chitosan composite was washed once with deionized water. All of the steps, the washing solutions, and the supernatant were collected, and the enzyme concentration was measured at 280 nm using a UV/Vis spectrophotometer (Shimadzu, Model 1601, Japan). The following formulas were used to determine the lysozyme loading capacity (LC) and encapsulation efficiency (EE) [39].

$$\mathrm{LC\%} = (\text{loaded amount of lysozyme} / \text{amount of chitosan composite}) \times 100 \quad (1)$$

$$\mathrm{EE\%} = [(\text{total lysozyme} - \text{unloaded lysozyme}) \times / \text{total lysozyme}] \times 100 \quad (2)$$

2.2.3 Composite characterization

2.2.3.1 SEM: Scanning electron microscopy (SEM) was used to investigate the composite's surface morphology. SEM was achieved using the TESCAN MIRA3 XMU model. SEM photos of the composite material were taken after it was coated with a thin layer of gold under reduced pressure.

2.2.3.2 ATR FTIR: FTIR spectroscopy was used to characterize the produced chitosan/PAA-PMA composite hydrogels. A spectrophotometer (Bruker Mode: Tensor II) with an attenuated total reflection accessory was used to make the measurements.

2.2.3.3 XRD: The chitosan/PAA-PMA composite hydrogels were analyzed using Cu radiation at 0.1546 nm at 40 kV and 40 mA in Panalytical Empyrean equipment. Scans were taken at temperatures ranging from 2 to 30 °C.

2.3 Assay of lysozyme and immobilized lysozyme activity

2.3.1 Assay of lysozyme activity: The spectrophotometric activities of free lysozyme and lysozyme-immobilized chitosan composite were investigated as follows: spectrophotometric analysis was used to measure the lysozyme activity at 620 nm. After addition of lysozyme, a culture of *M. lysodeikticus* cells suspended in phosphate buffer (0.1 M, pH 7.0) was observed for 5 min to determine the rate at which the optical density decreased. One enzyme unit (U) of lysozyme is defined as the quantity of enzyme that generates a 0.001 absorbance unit per minute change in OD 620 (at pH 7.0, 25 °C) [31]. All the experiments were carried out in triplicate.

2.3.2 Characterization of free and immobilized enzymes: Optimal temperature and pH were determined by individually changing the conditions of the lysozyme activity assay. An acetate buffer has a pH of 4.0–6.0, a phosphate buffer has a pH of 6.0–8.0, and a glycine-NaOH buffer has a pH of 8.0–9.0. Temperature effects on lysozyme and immobilized lysozyme were studied from 20 to 80 °C. The activities of lysozyme and immobilized lysozyme in various media were calculated as relative activity versus those seen under ideal reaction conditions.

2.4 Spectrophotometric determination of the chitosan composite–lysozyme interaction

In the absence and presence of various concentrations of chitosan and PAA-PMA (chitosan/acrylamide-maleic acid), the UV spectra of lysozyme in the region of 240–3420 nm were obtained using a UV–Vis spectrophotometer. After a sodium phosphate buffer baseline, lysozyme spectra were obtained after titration of chitosan/PAA-PMA. The changes in absorbance at 280 nm that resulted were recorded. All experiments were carried out in quartz cells with 0.1 mg/ml lysozyme and varied doses of chitosan/PAA-PMA suspension (0, 0.1, and 0.01 g) in 3 mL lysozyme solution [40].

2.5 Reusability of immobilized lysozyme

The reusability studies were performed in the lysozyme activity medium. The *M. lysodeikticus* cell suspension was removed from the chitosan composite after each activity measurement, and the cells were thoroughly washed before being re-suspended for the subsequent measurement. The same technique described above was used to measure the immobilized enzyme's activity.

2.6 Antimicrobial activity of free and immobilized lysozyme

The antimicrobial activity of chitosan/PAA-PMA (chitosan/acrylamide-maleicacid (K3)), Lys, and K3-Lys was investigated using the Kirby–Bauer disc diffusion assay against Gram-positive methicillin-resistant *Staphylococcus aureus* (MRSA) (ATCC 43300), *Enterococcus faecalis* (ATCC 29212), and Gram-negative *Pseudomonas aeruginosa* (ATCC) The test was performed according to the Clinical and Laboratory Standards Institute (CLSI) [41]. First, 100 µl of 10^7 CFU/mL bacterial suspension was spread on MHA and allowed to dry for about 10 min before the disks were placed on the plate. On the sterile blank disc, 20 µl of test solutions (10 mg/mL, dissolved in dimethyl sulfoxide solvent, DMSO) were dropped. At certain intervals, discs were placed on MHA inoculated with a bacteria isolate. The negative control was DMSO, while the positive controls were ciprofoxacin and linezolid antibiotics. All cultures were incubated at 37 °C for 24 h. After the incubation, the inhibition zone diameters were measured in terms of millimeters (mm) in diameter and evaluated. The diameter of the inhibition zone was classified as 6–10 mm (weak), 11–16 mm (moderate), and 17–25 mm (strong) [42].

2.7 Cytotoxicity assay

To evaluate cell viability, the XTT test was performed (Roche Diagnostic, Germany).

In 100 µL of DMEM culture fluid, cells were cultured at a density of 10^4 cells per well in 96-well plates and left to stick overnight. After 24 h, increasing concentrations of the drug (1000 µg/ml) were added to the two cell lines while maintaining the same final dose of the released composite, and the plates were incubated for another 24 h. The cells in the control groups were not given any treatment. 50 µl of XTT labeling solution was added to wells to identify living cells, and the plates were incubated at 37 °C for 4 h. After mixing, the absorbance of each well was measured at 450 nm and compared to the control using a microplate reader (Thermo, Germany). The viability of the cells was calculated as a percentage of the control (100 %) [43].

2.8 Statistical analysis

The experiments were performed at least three times, and the data were depicted as mean ± standard deviation (SD). Differences were considered statistically significant at a value of $p < 0.05$.

3 Results

The synthesized molecule includes maleic acid, which has carboxylic acid groups and needs to be used as a chelator. That is why this group is not used for lysozyme immobilization. Figure 1 shows the conjugation of chitosan composite to lysozyme between the activated carboxyl group of lysozyme and the amino groups of chitosan. The main advantage of this combination for enhanced antibacterial performance is due to the charge of lysozyme immobilized composite. At the last structure, there are carboxylate groups for metal binding, so these groups are occupied by metal ions, in addition lysozyme binding is via carboxyl group of lysoyzme, and so amino groups are functional.

3.1 SEM

SEM images of the synthesized chitosan composite were taken (Figure 2). The figure clearly shows that the chitosan composite has numerous pores for lysozyme adsorption.

3.2 FT-IR ATR

The FT-IR study was carried out to establish the existence of chitosan composite (K3) and lysozyme, as well as to look into potential interactions (Figure 3). In the previous work [37], we investigated the typical infrared absorption peaks of chitosan composite in depth. N–H stretching of free amino groups is responsible for the big peak at 3295 cm^{-1}, while C–H stretching is responsible for the absorption at 2961 cm^{-1}. Three separate mid-infrared zones are also included: amide I (1700–1600 cm^{-1}), amide II (1600–1500 cm^{-1}), and amide III

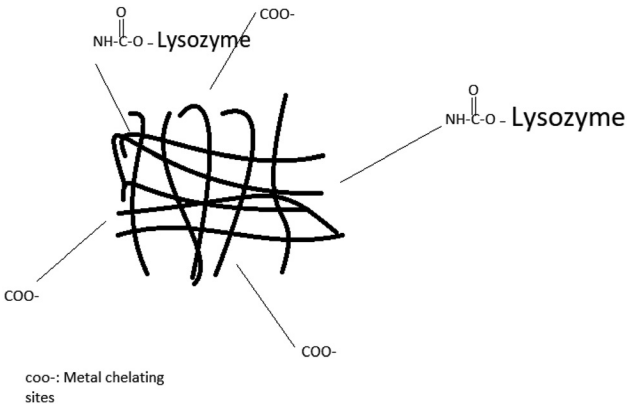

Figure 1: Schematic presentation of conjugation between chitosan composite and activated lysozyme.

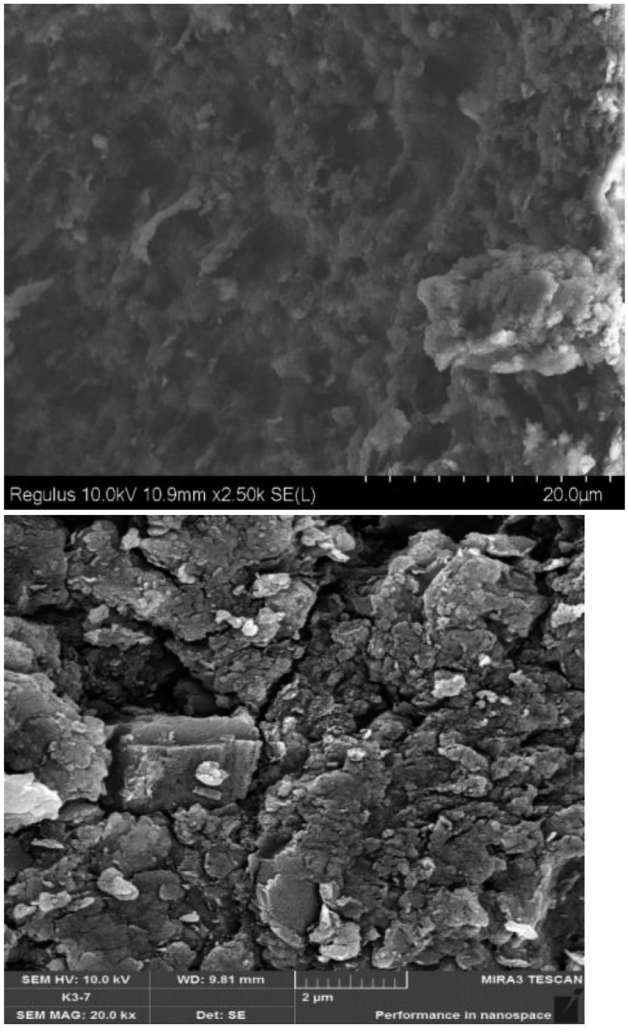

Figure 2: SEM image of freeze-dried chitosan composite (top), non-freeze-dried chitosan composite (bottom).

(1320–1230 cm^{-1}), where amide I was thought to have secondary structure interactions and the amide III signal was overlooked due to its weakness [44]. Thus, vibrations of the -helix's C=O stretching were assigned to the one centered at 1653 cm^{-1}, while N–H bending and C– N stretching were assigned to the one centered at 1538 cm^{-1} [45]. The FT-IR structure (Figure 3's blue line at the bottom) demonstrates lysozyme incorporation into the chitosan composite structure. Lysozyme is clearly seen to have adsorbed onto the chitosan composite. The lysozyme molecules are shown to be quite stable through secondary structures like the α-helical and β-sheets of the immobilized enzyme by the intensity ratio of the amide bands in both the purely lysozyme and the lysozyme immobilized onto the composite [46]. Additionally, these peaks do not differ from those of lysozyme, indicating that the lysozyme secondary structure has not changed after immobilization. The absorbance intensity of the amide II band is changed, but it is not so important to the conformation of the lysozyme [47].

3.3 Spectrophotometry determination of the chitosan composite–lysozyme interaction

Chitosan composites without lysozyme exhibited no absorption at the measured wavelengths of 240–340 nm, while after lysozyme loading they exhibited an obvious peak centered about 280 nm. This was designated as the typical absorption for lysozyme at various absorbance values (Figures 4a and b). The data showed that when lysozyme was added to the chitosan composite (K3), there was a slight hypsochromic shift due to lysozyme immobilization, as reported in the literature [7,48].

3.4 Lysozyme and immobilized lysozyme activity

For the next experiments for the immobilized enzyme research, at 50 °C temperature a lysozyme concentration of 1 mg/ml was selected. For immobilized enzyme, the ideal pH and temperature were found to be 7 and 50 °C, respectively. Free lysozyme exhibited activity at pH 6.5 and 50 °C. The enzyme, both in free and bound forms, was stored in 50 mM Tris buffer (pH 7.0) at 4 °C. The free enzyme samples retained their activity for 40 days, but the immobilized samples retained 80 % lysozyme activity on the 80th day. In terms

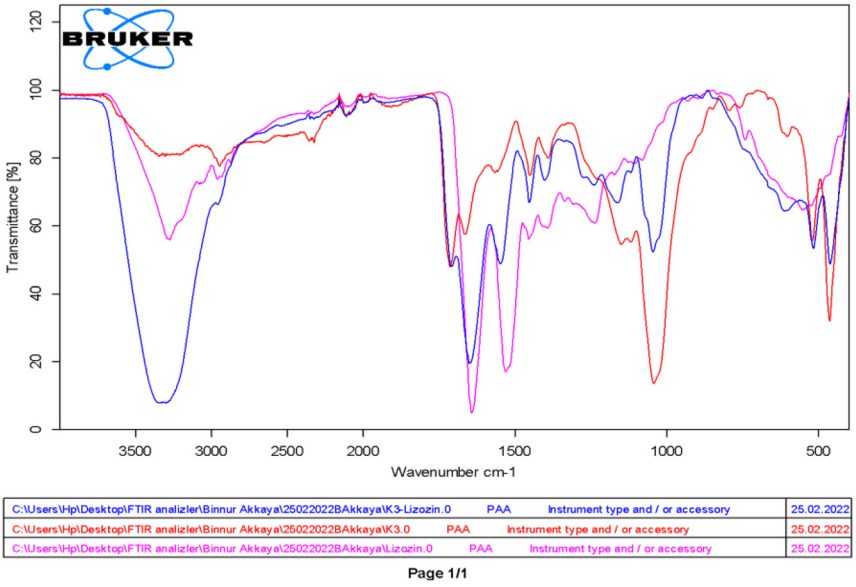

Figure 3: ATR FT-IR of chitosan composite, lysozyme and lysozyme immobilized chitosan composite (top to bottom).

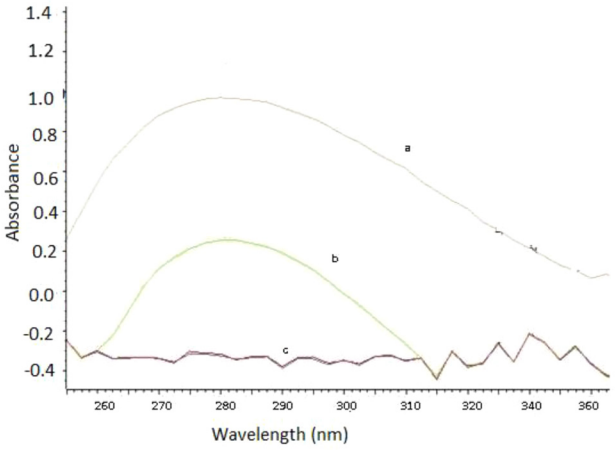

Figure 4: UV spectra (240–340 nm) of (a) lysozyme+0.01 g K3, (b) lysozyme + 0.05 g K3, (c) phosphate buffer + K3.

of thermostability, immobilization seems to improve the enzyme's shelf life (Figure 5). To summarize, the immobilization procedure for enzymes has little influence on the settings that can optimize their activity. It could be because of the conjugate coupling of chitosan amino groups on activated lysozyme (carboxyl groups) [49].

3.5 Resuability studies

The reusability results show that the covalently coupled lysozyme maintained approximately 86 % of its initial activity after 10 cycles (Figure 6).

3.6 Antimicrobial activity

According to the results of the disk diffusion method, it was determined that the K3 and K3- Lys compounds had a weak to moderate antibacterial activity on other microorganisms except MRSA (Table 1). Additionally, the inhibition zone diameters of K3-Lys remarkably increased to 120 % for *E. coli* and *Klebsiella pneumoniae*, 118 % for *P. aeruginosa*, and 113 % for *E. faecalis* of the initial level in the presence of Lys. Thus, K3-Lys had higher antimicrobial activities against bacteria than Lys based on inhibition zone diameters (Table 2) [5,48,50–52]. The compounds which were used for composite preparation (chitin, chitosan, carboxylic acid containing monomers) had antimicrobial activity [1,53–55].

Commonly employed in food, synthetic metal chelators increase the potency of antimicrobials such as lysozyme and prevent oxidative degradation. Metal chelators may enhance the antibacterial effect of food by reserving vital nutrients (such as iron) and/or removing cations that stabilize membranes (e.g., magnesium, calcium). Researchers reported that lysozyme and EDTA worked together to combat *E. coli* [33].

Metal-chelating substances (other than EDTA) showed synergy with lysozyme against a variety of bacteria; however, this synergy was not as strong as the synergy between EDTA and lysozyme. Multivalent cations, notably Fe^{2+} and Fe^{3+}, have been shown to exhibit a preference for EDTA. Because carboxylic acid-containing materials, such as poly (acrylic acid), chelate metal ions through electrostatic interactions rather than high affinity metals attaching to specific ligands. There was a theory that the

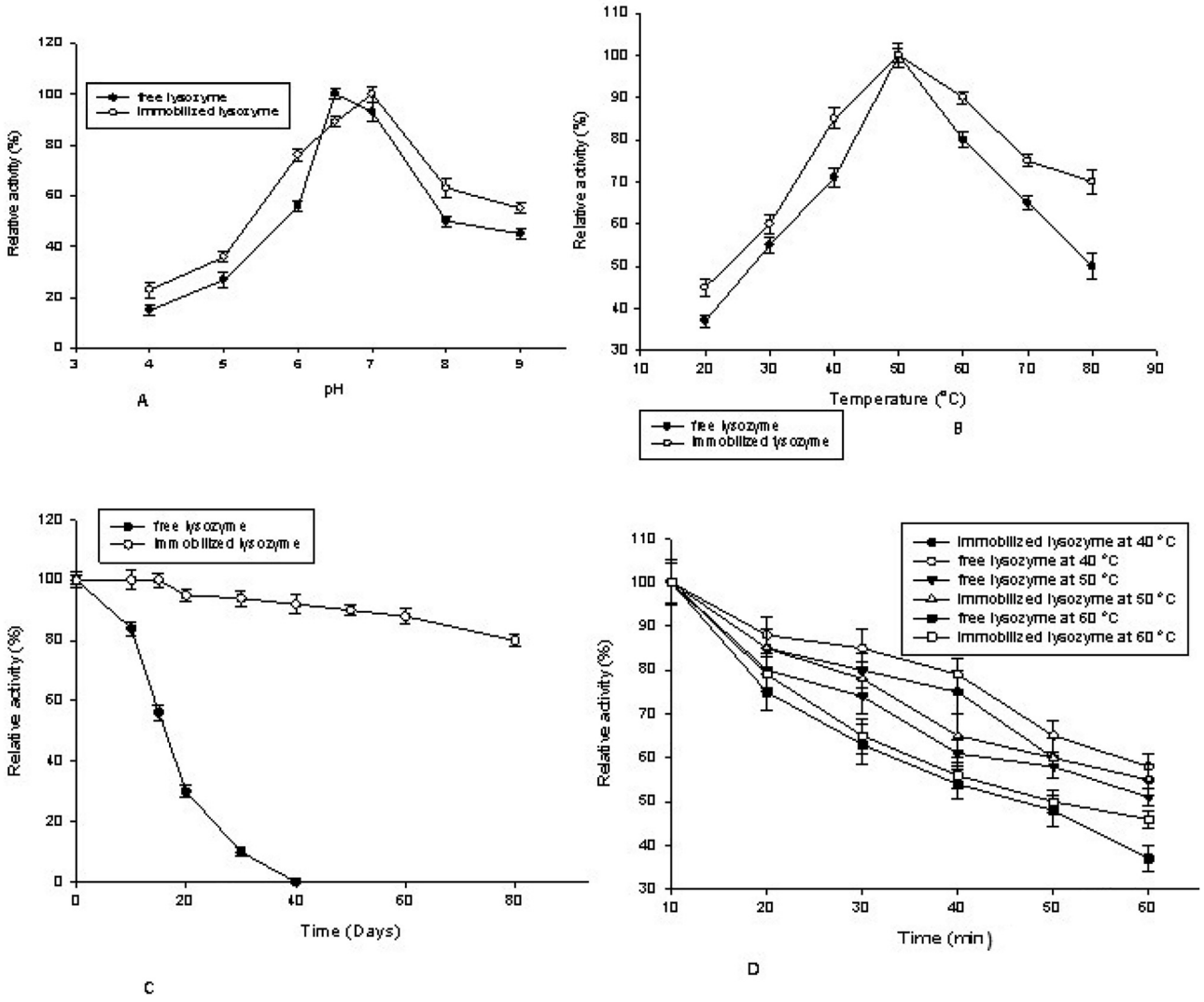

Figure 5: Assesment of free and immobilized lysozyme. (A) Influence of pH on the activities of free and immobilized lysozyme. (B) Optimal temperature for free and immobilized lysozyme. (C) Effect of storage. (D) Thermal stability of free lysozyme and immobilized lysozyme.

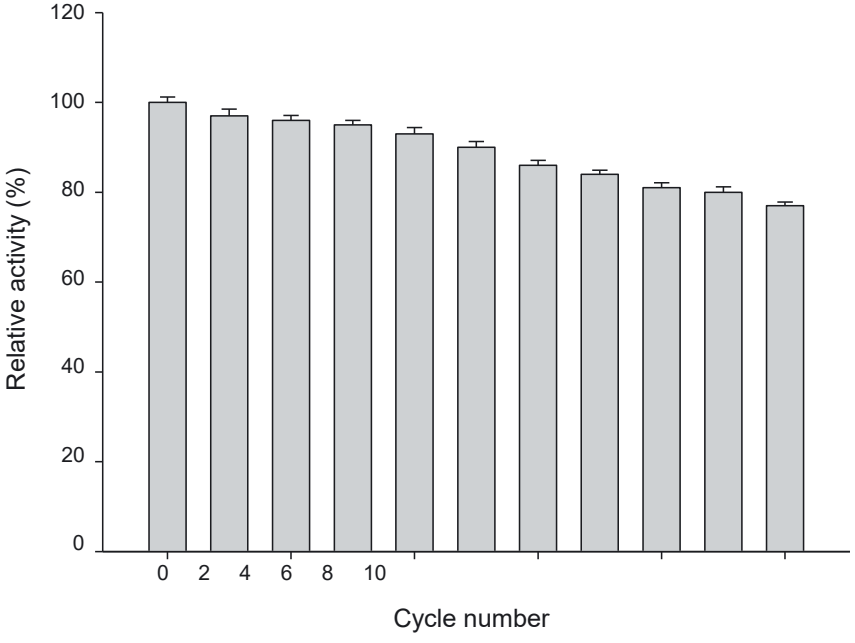

Figure 6: Reusability performance of immobilized lysozyme.

Table 1: Antibacterial activity of synthesized compounds.

Treatment group	Inhibition zone (mm)				
	Escherichia coli	*Klebsiella pneumoniae*	*Pseudomonas aeruginosa*	*Enterococcus faecalis*	*Staphylococcus aureus*
K_3	8 ± 1.5	8 ± 1.2	9 ± 0.5	13 ± 0.7	R
Lys	R	R	R	R	R
K_3-Lys	10 ± 1.7	10 ± 1.3	11 ± 0.4	15 ± 0.8	R

K3-Lys (lysozyme concentration: 1 mg/mL) suspension against pathogen ATCC strains in DMSO K3 and K3-Lys are at a concentration of 10 mg/mL. R, resistant. DMSO was used as a negative control.

Table 2: Literature comparison with zone diameter of some microorganisms and immobilized lysozyme.

Treatment group	Inhibition zone (mm) antibacterial properties					References
	Escherichia coli	*Klebsiella pneumoniae*	*Pseudomonas aeruginosa*	*Enterococcus faecalis*	*Staphylococcus aureus*	
CS	R					[48]
CS-NPs	10.34 ± 1.21					
CS-Lys-NPs	13.11 ± 0.48					
CS/ALG	–	–	6	9	12	[50]
β-CS	3.34 ± 0.71					[51]
Lys	3.71 ± 0.38					
Lys loaded LMW *β*-CS NPs	11.69 ± 1.41					
CNCs stabilized Lys loaded LMW *β*-CS NPs	13.29 ± 1.38					
Lys					7.03	[5]
LQC NPs					9.48	
HQC NPs					11.34	
CNC stabilized LQC NPs					12.40	
CNC stabilized HQC NPs					12.55	
CNC stabilized Lys loaded LQC NPs					13.43	
CNC stabilized Lys loaded HQC NPs					14.32	
Surface-grafted chitosan with immobilized lysozyme					High antimicrobial activity	[52]
N-succinyl chitosan immobilized lysozyme					12.3	[56]
K_3	8 ± 1.5	8 ± 1.2	9 ± 0.5	13 ± 0.7	R	This study
Lys	R	R	R	R	R	
K_3-Lys	10 ± 1.7	10 ± 1.3	11 ± 0.4	15 ± 0.8	R	

reduced synergistic effect of lysozyme with metal chelating materials resulted from the competitive binding of large, positively charged molecules, such as lysozyme, by negatively charged metal chelating materials [33].

Apart from carboxylic groups, immobilization of lysozyme increased synergistic effects in the current study. So immobilized lysozyme and metal-chelating carboxylic groups both show synergistic antimicrobial activity. At pH 7.0, carboxylic acid groups are deprotonated and should bind to metal ions. At the same pH conditions, immobilized lysozyme shows enhanced antimicrobial activity [57].

Along with calcium, magnesium helps Gram-negative bacteria bind polysaccharides on their surfaces by cross-linking negatively charged groups to form salt bridges. Magnesium and calcium can create metal complexes that can cause cell solute leakage and viability loss. The growth, replication, respiration, and DNA synthesis processes in bacterial cells all require iron. Such crucial cations being chelated from the lipopolysaccharides (LPS) layer may compromise its structural or functional integrity, allowing lysozyme to enter the cell wall [17,18].

With this study, we succeeded in effectively coexisting lysozyme and metal chelating groups together in the same

composite by preventing lysozyme binding to carboxylate groups of maleic acid which is necessary for metal binding. Metal binding and shielding of carboxylate groups by metal binding, lysozyme immobilization, all of these properties make the lysozyme immobilized composite efficient.

Chitosan take important place in this composite. The electrostatic interactions between the polycationic structure of chitosan and the anionic groups on the bacterial cell surface, which result in the alteration of the cell wall (Gram-positive) or outer membrane (Gram-negative), appear to play a key role in the antibacterial activity of chitosan and its derivatives. Charge, molecular weight and the physical state of chitosan, environment and kind of microorganisms also affect the antimicrobial activity of material. So the synergistic effect of chitosan on lysozyme antimicrobial activity is obvious [58].

Antibacterial activity of chitosan-lysozyme conjugation is studied by other researchers. In contrast, lysozyme selectively targets particular sites of the glycosidic linkages between the N-acetylhexosamines of the peptidoglycan layer in bacterial cell walls. Lysozyme generally has a difficult time attacking the walls of Gram-positive bacteria. Due to the outer membrane's exclusion of lysozyme and impediment to its entry to the site of action on the peptidoglycan in cell walls, Gram-negative bacteria are less vulnerable to such an attack [59].

In contrast to poisonous capping agents like cetyltrimethylammonium bromide (CTAB) and hexadecyltrimethylammonium chloride (CTAC), chitosan (CS), which is green and nontoxic, plays a key function as a shape-directing agent [60]. This property of chitosan is also important for gaining antimicrobial activity.

3.7 Cell viability test

Using the mouse fibroblast cell line L929, the cytotoxicity of chitosan composite (K3) and lysozyme immobilized chitosan composite (K3-lys) was investigated. The vitality of cell lines was determined after 12 and 24 h of treatment with both composites. After 24 h, the chitosan composite and lysozyme immobilized chitosan composite demonstrated.

98.42 and 101.03 %, respectively. These findings indicate that the chitosan composite and lysozyme immobilized chitosan composite are not cytotoxic (Figure 7).

4 Conclusions

Evaluating the antimicrobial activity of the active components was done using especially *E. coli* and *S. aureus* as examples of Gram-positive and Gram-negative bacteria, respectively [61–63]. Synthetic metal chelator chitosan composites were successfully prepared, and lysozyme immobilization was achieved by the covalent crosslinking (EDAC) process. Lysozyme and immobilized lysozyme had higher antimicrobial activity against *E. coli, K. pneumoniae, P. aeruginosa, E. faecalis, and S. aureus* than free lysozyme. The cytotoxic effects of both of them were investigated, but

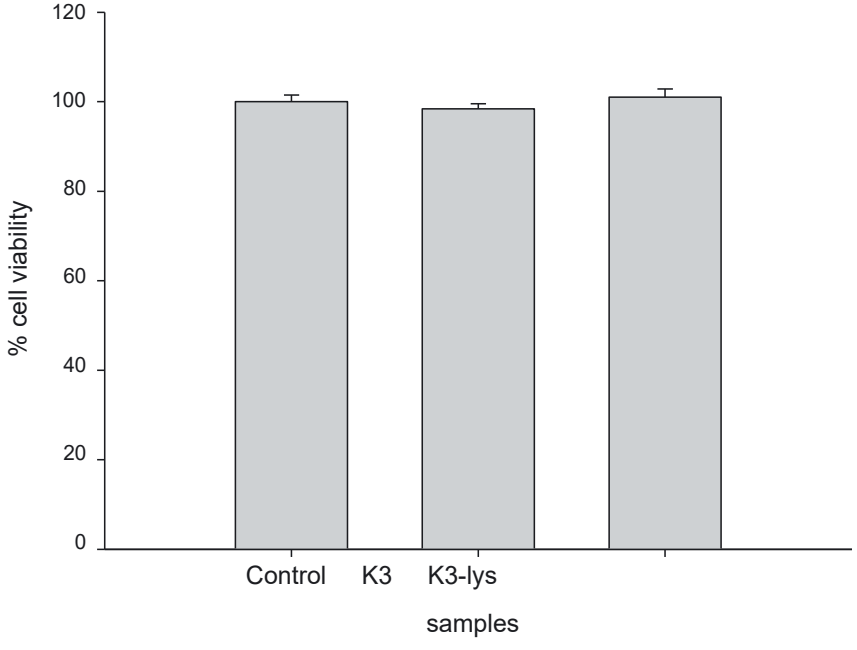

Figure 7: Cell viability test.

there was no cytotoxic effect. This work demonstrated an improved antibacterial method that makes use of synthetic metal chelators and lysozyme immobilization, gaining both properties and providing a novel idea for the creation of superior antibacterial composite materials used in the food and medicine industries in future studies such as food packaging and tissue engineering, respectively.

Author contributions: All the authors have accepted responsibility for the entire content of this submitted manuscript and approved submission.

Research funding: This article was supported by CUBAP (project number F-2022-656).

Conflict of interest statement: The authors declare that they have no conflicts of interest regarding this article.

References

1. Jiang S., Qin Y., Yang J., Li M., Xiong L., Sun Q. Enhanced antibacterial activity of lysozyme immobilized on chitin nanowhiskers. *Food Chem*. 2017, *221*, 1507–1513.
2. Li H., Gao C., Tang L., Wang C., Chen Q., Zheng Q., Yang S., Sheng S., Zan X. Lysozyme (Lys), tannic Acid (TA), and graphene oxide (GO) thin coating for antibacterial and enhanced osteogenesis. *ACS Appl. Bio. Mater.* 2020, *3*, 673–684.
3. He L., Cui Y., Zhang C. The corrosion resistance, cytotoxicity, and antibacterial properties of lysozyme coatings on orthodontic composite arch wires. *RSC Adv*. 2020, *10*, 18131–18137.
4. Esmaeilnejad-Ahranjani P., Maboudi S. A. Tuning the size and concentration of functional molecules coated onto mesoporous silica nanoparticles for efficient therapeutic protein delivery. *Mater. Today Commun.* 2023, *35*, 105632.
5. Chang S., Zou X., Zhu B., You B., You L., Zhao Z., Hileuskaya K. The characteristics of polysaccharide from *Gracilaria chouae* and its application in food packaging with carboxymethyl cellulose and lysozyme. *Food Hydrocoll.* 2023, *135*, 108109.
6. Cerón A. A., Nascife L., Costa S. A., Oliveira do Nascimento J. S., Morisso F. D. P., Baruque-Ramos J., Oliveire R. C., Costa S. M. Synthesis of chitosan-lysozyme microspheres, physicochemical characterization, enzymatic and antimicrobial activity. *Int. J. Biol. Macromol.* 2021, *185*, 572–581.
7. Zhang H., Qiu T., Bai Y., Chen B., Yan J., Xu J. Enhanced antibacterial activity of lysozyme loaded quaternary ammonium chitosan nanoparticles functionalized with cellulose nanocrystals. *Int. J. Biol. Macromol.* 2021, *191*, 71–78.
8. Wang Y., Li S., Jin M., Han Q., Liu S., Chen X., Han Y. Enhancing the thermo-stability and anti-bacterium activity of lysozyme by immobilization on chitosan nanoparticles. *Int. J. Mol. Sci.* 2020, *21*, 1635.
9. Eivazzadeh-Keihan R., Radinekiyan F., Maleki A., Bani M. S., Hajizadeh Z., Asgharnasl S. A novel biocompatible core-shell magnetic nanocomposite based on cross- linked chitosan hydrogels for in vitro hyperthermia of cancer therapy. *Int. J. Biol. Macromol.* 2019, *140*, 407–414.
10. Huang T., Qian Y., Wei J., Zhou C. Polymeric antimicrobial food packaging and its applications. *Polymers* 2019, *11*, 560.
11. Lago M. A., Sendón R., de Quirós A. R. B., Sanches-Silva A., Costa H. S., Sánchez- Machado D. I., Valdez H. S., Angulo I., Aurrekoetxea G. P., Torrieri E., Lopez-Cervantes J., Paseiro P. Preparation and characterization of antimicrobial films based on chitosan for active food packaging applications. *Food Bioproc.* 2014, *7*, 2932–2941.
12. Ojagh S. M., Rezaei M., Razavi S. H., Hosseini S. M. H. Development and evaluation of a novel biodegradable film made from chitosan and cinnamon essential oil with low affinity toward water. *Food Chem*. 2010, *122*, 161–166.
13. Kanatt S. R., Rao M. S., Chawla S. P., Sharma A. Active chitosan-polyvinyl alcohol films with natural extracts. *Food Hydrocoll.* 2012, *29*, 290–297.
14. Siripatrawan U., Noipha S. Active film from chitosan incorporating green tea extract for shelf life extension of pork sausages. *Food Hydrocoll.* 2012, *27*, 102–108.
15. Yu Z., Li B., Chu J., Zhang P. Silica in situ enhanced PVA/chitosan biodegradable films for food packages. *Carbohydr. Polym.* 2018, *184*, 214–220.
16. Arkoun M., Daigle F., Heuzey M. C., Ajji A. Mechanism of action of electrospun chitosan-based nanofibers against meat spoilage and pathogenic bacteria. *Molecules* 2017, *22*, 585.
17. Boland J. S., Davidson P. M., Bruce B., Weiss J. Cations reduce antimicrobial efficacy of lysozyme-chelator combinations. *J. Food Prot.* 2004, *67*, 285–294.
18. Boland J. S., Davidson P. M., Weiss J. Enhanced inhibition of Escherichia coli O157: H7 by lysozyme and chelators. *J. Food Prot.* 2003, *66*, 1783–1789.
19. Branen J. K., Davidson P. M. Enhancement of nisin, lysozyme, and monolaurin antimicrobial activities by ethylenediaminetetraacetic acid and lactoferrin. *Int. J. Food Microbiol.* 2004, *90*, 63–74.
20. Cannarsi M., Baiano A., Sinigaglia M., Ferrara L., Baculo R., Del Nobile M. A. Use of nisin, lysozyme and EDTA for inhibiting microbial growth in chilled buffalo meat. *Int. J. Food Sci. Technol.* 2008, *43*, 573–578.
21. Davidson P. M., Taylor T. M., Schmidt E. S. Chemical preservatives and natural antimicrobial compounds. *Food Microbiol. Fundam. Front.* 2007, *33*, 713–745.
22. Dong R., Lindau M., Ober C. K. Dissociation behavior of weak polyelectrolyte brushes on a planar surface. *Langmuir* 2009, *25*, 4774–4779.
23. Gill A. O., Holley R. A. Surface application of lysozyme, nisin, and EDTA to inhibit spoilage and pathogenic bacteria on ham and bologna. *J. Food Prot.* 2000, *63*, 1338–1346.
24. Wei Z., Wu S., Xia J., Shao P., Sun P., Xiang N. Enhanced antibacterial activity of hen egg-white lysozyme against *Staphylococcus aureus* and *Escherichia coli* due to protein fibrillation. *Biomacromolecules* 2021, *22*, 890–897.
25. Ghasemzadeh M. A., Nasrollahi S. M. H., Zolfaghari M. R. Synthesis and antibacterial evaluation of some new 1,4-dihydropyridines in the presence of Fe3O4@silica sulfonic acid nanocomposite as catalyst. *Acta Chim. Slov.* 2018, *65*, 199–207.
26. Wang Z., Yu H., Ma K., Chen Y., Zhang X., Wang T., Li S., Zhu X., Wang X. Flower-like surface of three-metal-component layered double hydroxide composites for improved antibacterial activity of lysozyme. *Bioconjugate Chem*. 2018, *29*, 2090–2099.
27. Nakimbugwe D., Masschalck B., Atanassova M., Zewdie-Bsüner A., Michiels C. W. Comparison of bactericidal activity of six lysozymes at atmospheric pressure and under high hydrostatic pressure. *Int. J. Food Microbiol.* 2006, *108*, 355–363.

28. Sanaei- Rad S., Ghasemzadeh M. A., Aghaei S. S. Synthesis and structure elucidation of ZnFe2O4/IRMOF-3/GO for the drug delivery of tetracycline and evaluation of their antibacterial activities. *J. Organomet. Chem.* 2022, *960*, 122221.
29. Singh B. P., Rohit M. K. M., Sharma R., Bhushan B., Ghosh S., Goel G. Nano-conjugated food-derived antimicrobial peptides as natural biopreservatives: a review of technology and applications. *Antibiotics* 2023, *2*, 244.
30. Ghasemzadeh M. A., Abdollahi-Basir M. H., Elyasi Z. Synthesis of some novel imidazoles catalyzed by Co3O4 nanoparticles and evaluation of their antibacterial activities. *Comb. Chem. High Throughput Scree.* 2018, *21*, 271–280.
31. Ben Braïek O., Morandi S., Cremonesi P., Smaoui S., Hani K., Ghrairi T. Safety, potential biotechnological and probiotic properties of bacteriocinogenic Enterococcus lactis strains isolated from raw shrimps. *Microb. Pathog.* 2018, *117*, 109–117.
32. Tian F., Decker E. A., Goddard J. M. Control of lipid oxidation by nonmigratory active packaging films prepared by photoinitiated graft polymerization. *J. Agric. Food Chem.* 2012, *60*, 7710–7718.
33. Roman M. J., Decker E. A., Goddard J. M. Metal-chelating active packaging film enhances lysozyme inhibition of Listeria monocytogenes. *J. Food Prot.* 2014, *77*, 1153–1160.
34. Peksen Ozer B. B., Uz M., Oymaci P., Alsoy Altinkaya S. Development of a novel strategy for controlled release of lysozyme from whey protein isolate based active food packaging films. *Food Hydrocoll.* 2016, *61*, 877–886.
35. Mahmud J. A., Hasannuzzaman M., Nahar K., Rahman A., Hossain M. S., Fujita M. Maleic acid assisted improvement of metal chelation and antioxidant metabolism confers chromium tolerance in Brassica juncea L. *Ecotoxicol. Environ. Saf.* 2017, *144*, 216–226.
36. Abd El-Ghaffar M., Elhalawany N., Ahmed E., Sabaa M. Synthesis and characterization of some chelating polymers bearing maleic acid and/or sodium maleate moieties for removal of some toxic heavy metal ions. *Clean Technol. Environ. Policy* 2013, *15*, 1013–1021.
37. Akkaya R., Akkaya B., Taşkın Çakıcı G. Chitosan-poly (acrylamide-co-maleic acid) composite synthesis, characterization, and investigation of protein adsorption behavior. *Polym. Bull.* 2022, *80*, 1–16.
38. Wang J., Tang L., Somasundaran P., Fan W., Zeng G., Deng Y., Zhou Y., Wang J., Shen Y. Highly effective antibacterial activity by the synergistic effect of three dimensional ordered mesoporous carbon-lysozyme composite. *J. Colloid Interface Sci.* 2017, *503*, 131–141.
39. Çetin K., Aslıyüce S., Idil N., Denizli A. Preparation of lysozyme loaded gelatin microcryogels and investigation of their antibacterial properties. *J. Biomater. Sci. Polym. Edition* 2021, *32*, 189–204.
40. Shareghi B., Farhadian S., Zamani N., Salavati-Niasari M., Gholamrezaei S. Stability and enzyme activity of lysozyme in the presence of Fe_3O_4 nanoparticles. *Monatsh. Chem*. 2016, *147*, 465–471.
41. CLSI. *Performance Standards for Antimicrobial Susceptibility Testing*, 30th ed; M100, Clinical and Laboratory Standards Institute: Wayne, PA, USA, 2020.
42. Arasoglu T., Derman S., Mansuroglu B., Yelkenci G., Kocyigit B., Gumus B., Acar T., Kocacaliskan I. Synthesis, characterization and antibacterial activity of juglone encapsulated PLGA nanoparticles. *J. Appl. Microbiol.* 2017, *123*, 1407–1419.
43. Joha Z., Yulak F., Öztürk A., Şahin B., Yıldırım Ş. The anticancer effect of cannabinoid 2 agonist L-759,633 on C6 and SH-SY5Y cell lines. *Turk. J. Sci. Health* 2021, *2*, 6–13.
44. Pelton J. T., McLean L. R. Spectroscopic methods for analysis of protein secondary structure. *Anal. Biochem.* 2000, *277*, 167–176.
45. Barth A. Infrared spectroscopy of proteins. *Biochim. Biophys. Acta* 2007, *1767*, 1073–1101.
46. Lawrence G., Baskar A. V., El-Newehy M. H., Cha W. S., Al-Deyab S. S., Vinu A. Quick high-temperature hydrothermal synthesis of mesoporous materials with 3D cubic structure for the adsorption of lysozyme. *Sci. Technolo. Adv. Mater.* 2015, *16*, 024806.
47. Ernest V., Gajalakshmi S., Mukherjee A., Chandrasekaran N. Enhanced activity of lysozyme-AgNP conjugate with synergic antibacterial effect without damaging the catalytic site of lysozyme. *Artif. Cells Nanomed. Biotechnol.* 2014, *42*, 336–343.
48. Wu T., Wu C., Fu S., Wang L., Yuan C., Chen S., Hu Y. Integration of lysozyme into chitosan nanoparticles for improving antibacterial activity. *Carbohydr. Polym.* 2017, *155*, 192–200.
49. Yamada H., Imoto T., Fujita K., Okazaki K., Motomura M. Selective modification of aspartic acid-101 in lysozyme by carbodiimide reaction. *Biochemistry* 1981, *20*, 4836–4842.
50. Thaya R., Vaseeharan B., Sivakamavalli J., Iswarya A., Govindarajan M., Alharbi N. S., Kadaikunnan S., Al-Anbr M. N., Khaled J. M., Benelli G. Synthesis of chitosan-alginate microspheres with high antimicrobial and antibiofilm activity against multi-drug resistant microbial pathogens. *Microb. Pathog.* 2018, *114*, 17–24.
51. Zhang H., Feng M., Chen S., Shi W., Wang X. Incorporation of lysozyme into cellulose nanocrystals stabilized β-chitosan nanoparticles with enhanced antibacterial activity. *Carbohydr. Polym.* 2020, *236*, 115974.
52. Yuan S., Yin J., Jiang W., Liang B., Pehkonen S. O., Choong C. Enhancing antibacterial activity of surface-grafted chitosan with immobilized lysozyme on bioinspired stainless steel substrates. *Colloids Surf. B: Biointerfaces* 2013, *106*, 11–21.
53. Gratzl G., Paulik C., Hild S., Guggenbichler J. P., Lackner M. Antimicrobial activity of poly (acrylic acid) block copolymers. *Mater. Sci. Eng. C Mater. Biol. Appl.* 2014, *38*, 94–100.
54. Ferrer-Luque C. M., Arias-Moliz M. T., González-Rodríguez M. P., Baca P. Antimicrobial activity of maleic acid and combinations of cetrimide with chelating agents against Enterococcus faecalis biofilm. *J. Endod.* 2010, *36*, 1673–1675.
55. Kim S., Fan J., Lee C. S., Lee M. Dual functional lysozyme-chitosan conjugate for tunable degradation and antibacterial activity. *ACS Appl. Bio Mater.* 2020, *3*, 2334–2343.
56. Niu X., Zhu L., Xi L., Guo L., Wang H. An antimicrobial agent prepared by *N*-succinyl chitosan immobilized lysozyme and its application in strawberry preservation. *Food Control* 2020, *108*, 106829.
57. Wang P., Zhang C., Zou Y., Li Y., Zhang H. Immobilization of lysozyme on layer-by- layer self-assembled electrospun films: characterization and antibacterial activity in milk. *Food Hydrocoll.* 2021, *113*, 106468.
58. Confederat L. G., Tuchilus C. G., Dragan M., Sha 'at M., Dragostin O. M. Preparation and antimicrobial activity of chitosan and its derivatives: a concise review. *Molecules* 2021, *36*, 3694.
59. Song Y., Babiker E., Usui M., Saito A., Kato A. Emulsifying properties and bactericidal action of chitosan–lysozyme conjugates. *Food Res. Int.* 2002, *35*, 459–466.

60. Zhang W., Taheri-Ledari R., Ganiali F., Mirmohammadi S. S., Qazi F. S., Saeidirad M., KashtiAray A., Zarei-Shokat S., Tian Y., Maleki A. Effects of morphology and size of nanoscale drug carriers on cellular uptake and internalization process: a review. *RSC Adv*. 2023, *13*, 80–114.
61. Westlake J. R., Tran M. W., Jiang Y., Zhang X., Burrows A. D., Xie M. Biodegradable active packaging with controlled release: principles, progress, and prospects. *ACS Food Sci. Technol.* 2022, *2*, 1166–1183.
62. Erol K., Tatar D., Veyisoğlu A., Tokatlı A. Antimicrobial magnetic poly (GMA) microparticles: synthesis, characterization and lysozyme immobilization. *J. Polym. Eng.* 2021, *41*, 144–154.
63. Ahghari M. R., Soltaninejad V., Maleki A. Synthesis of nickel nanoparticles by a green and convenient method as a magnetic mirror with antibacterial activities. *Sci. Rep.* 2020, *10*, 12627.